The Temperature Dependence of Isothermal Moisture vs. Potential Characteristics of Soils[1]

J. R. NIMMO AND E. E. MILLER[2]

ABSTRACT

A method has been developed for rapid, transient measurement of hysteretic soil-moisture characteristics as a function of temperature. While a varying soil-water pressure was imposed on a thin sample by means of flexible membranes held in firm contact with the soil, water content was measured by gamma-ray attenuation, and matric potential was measured with tensiometers. The applied pressure was cycled through a program designed to obtain hysteretic $\theta(\psi)$ main and scanning curves. Isothermal characteristics were measured for 181-μm glass beads, Plainfield (Typic Udipsamments) sand, and an undisturbed core of Plano (Typic Argiudolls) silt loam at several temperatures in the 4° to 50°C range. At each temperature the measurements included main drying and wetting curves covering the θ range from 0.30 to 0.05 m^3 water/m^3 for glass beads, 0.30 to 0.17 for sand, and 0.45 to 0.37 for silt loam. A model has been developed to quantify the temperature dependence as a function of θ. Combined with an isothermal hysteresis model of Mualem, this model requires only three characteristic functions to represent all hysteretic $\theta(\psi)$ curves for a given medium at all temperatures. Model calculations for the sand and silt loam data indicate that except near saturation, the temperature effect is greater than can be accounted for by the temperature dependence of the surface tension of pure water. The results rule out several possible explanations but they support the hypothesis that the concentration and effectiveness of dissolved surfactants increases with temperature.

Additional Index Words: **hysteresis, transient characteristics, glass beads, undisturbed core, soil-moisture membranes, model, surface tension, surfactant.**

Nimmo, J.R., and E.E. Miller. 1986. The temperature dependence of isothermal moisture vs. potential characteristics of soils. Soil Sci. Soc. Am. J. 50:1105–1113.

MANY EXPERIMENTERS, beginning with King (1892), have shown that the moisture-holding capacity of soil is significantly influenced by temperature. Briggs (1897) proposed that the temperature dependence of the surface tension of water was responsible for such effects. Considered quantitatively as the scaling of matric potential ψ in proportion to surface tension σ, this mechanism constitutes one part of the surface-tension, viscous-flow (STVF) concept of moisture behavior in granular porous media (Miller and Miller, 1956). Philip and de Vries (1957) expressed it for a given water content θ as

$$(\partial\psi/\partial T)/\psi = (\partial\sigma/\partial T)/\sigma \qquad [1]$$

where T is temperature. Over the temperature range of chief concern in soil physics, the thermal coefficient of surface tension $(\partial\sigma/\partial T)/\sigma$ for pure water is nearly constant at -2.1×10^{-3} °C^{-1}.

R. Gardner (1955) and Taylor and Stewart (1960) undertook direct measurements of the change in ψ with constant θ, using a method originated by Moore (1940). Measuring ψ with tensiometers in small soil samples while the temperature of the samples was varied with no water flow in or out of the system, these investigators found that the temperature dependence of ψ was greater than the STVF prediction by an order of magnitude or more. Unfortunately, these measurements were subject to at least two unintended influences. First, there was the possibility of thermal expansion of air bubbles entrapped in the soil water, an effect first noted by Bouyoucos (1915). Second, there were variations in θ that occur when Hg manometers are used in situations where volumes of water exchanged through tensiometers are significant compared to the quantity of soil. Jury and Miller (1974) performed a similar experiment using improved techniques. Draining from a sample that had been packed under water assured that air entrapment would be negligible, and the use of a strain-gage transducer permitted ψ measurements without significant changes in θ. For their sample of medium sand, Jury and Miller obtained values of $\partial\psi/\partial T$ up to five times greater than would be predicted on the basis of surface tension.

Another way to eliminate the influence of entrapped air expansion is to perform several experiments isothermally, each at a different temperature. Taylor (1958), Wilkinson and Klute (1962), Meeuwig (1964), and Constantz (1982, 1983) have measured the temperature dependence of ψ-θ curves in this way, using the standard pressure plate and similar methods involving equilibrium at each ψ value. Temperature dependences observed with these techniques show a pronounced texture dependence: for coarse soil (e.g., the coarse sand sample of Wilkinson and Klute) the dependence is about as strong as expected from the surface tension hypothesis, while for fine-textured soils it is significantly stronger. Constantz (1983) also observed that the temperature dependence increased with dryness of soil.

Destructive methods, permitting accurate gravimetric θ measurements but requiring the use of different samples at different temperatures, have also been used to obtain the temperature dependence of $\psi(\theta)$ at equilibrium. Chahal (1964) performed such experiments with a fine silt, correcting for the expansion of entrapped air where necessary, and found close agreement with the STVF model. Vetterlein (1968) measured $\psi(\theta)$ at different temperatures using replicate samples of eight soils of widely varying textures, finding in nearly every case that there was no significant temperature trend. These experiments are not a good basis for generalization because, as Vetterlein noted, variability among the samples can easily overwhelm the temperature dependence.

Several experimenters have studied the effect of either transient or steady-state flow on the tempera-

[1] Contribution from Water Resources Div., U.S. Geological Survey, Menlo Park, CA, and Dep. of Physics and Dep. of Soil Science, Univ. of Wisconsin-Madison. Done in part while the senior author was a graduate student in Physics at the Univ. of Wisconsin-Madison. Research supported in part by the Wisconsin Water Resources Center, the Wisconsin Alumni Research Foundation, and the U.S. Dep. of Agric. (Hatch formula funds project 142-UW-2607). Received 5 Aug. 1985.

[2] Physicist, U.S. Geological Survey, Water Resources Div., 345 Middlefield Rd., Menlo Park, CA 94025; Professor, Dep. of Physics and Dep. of Soil Science, Univ. of Wisconsin-Madison, Madison, WI 53706.

ture dependence of ψ-θ curves, obtaining results similar to those of equilibrium studies. Using replicate samples at different temperatures, Flocker et al. (1968) found no significant temperature trend except when the soil was fairly dry. Using the same samples at different temperatures under both transient and steady-state conditions, Haridasan and Jensen (1972) found that temperature dependences were several times greater than predicted by the STVF hypothesis. With measurements under transient conditions in a nearly monodispersed sand fraction, Crausse et al. (1981) obtained no significant deviation from surface-tension predictions, in agreement with the findings of Wilkinson and Klute (1962) for the same type of medium.

Cary (1975) investigated the effect of temperature on soil-moisture hysteresis by measuring θ as ψ was adjusted through drying and wetting cycles. The results, presented as the areas of hysteresis loops at 5° and 15°C, show a significant temperature effect only for a silty clay, the finest of three textures used in the experiment. Cary's data do not permit separate comparisons of drying and wetting curves with theory.

The experimental evidence cited here supports several generalizations concerning the temperature dependence of the ψ-θ relation in soils. Except for measurements on coarse soils, the results indicate a greater temperature dependence than the STVF model alone can explain. In some cases the magnitude of the temperature dependence has been found to vary with moisture content, being greater in drier soils. Where the temperature dependence has been measured under either transient or steady-state flow conditions, results have not been significantly different from those of equilibrium experiments.

The only major theoretical treatment of this topic is that of Peck (1960), which considered the combined effects of surface tension and entrapped air. Applying the ideal gas law to a constant number of equal-sized bubbles and taking account of the temperature dependence of σ, Peck derived a formula for $\partial\psi/\partial T$ that had the effect of adding two new terms to the right-hand side of Eq. 1. Using reasonable assumptions for the amount of air entrapped, Peck predicted a temperature dependence several times larger than that due to surface tension alone.

Other mechanisms suggested to account for these deviations include the influence of temperature on contact angle, on the swelling of clay particles, and on the effect of surfactants contained in soil water. Little theoretical development of such mechanisms has been published.

The present study was designed to measure and interpret the temperature dependence of hysteretic moisture characteristics for both natural and artificial soils over the temperature range important in the field. For the clearest comparison with the simple STVF model, these objectives are best met by a series of isothermal experiments. A rapid, transient method was chosen in order to accumulate a complete set of data with each sample quickly enough to miniimize any significant aging effects. This choice provides resemblance to rapid changes that occur in the field, especially during infiltration and redistribution. Drying, wetting, and scanning curves were measured so that any differences due to direction of moisture change might be apparent. The effect of temperature was quantified according to a simple scheme that shows its variation with water content and provides a basis for appraising various hypothetical mechanisms of temperature dependence.

EXPERIMENT

The original experimental design was based on the flow-cell method of Richards (1931) as developed into a transient system for use with glass beads by Topp and Miller (1966) and Bomba (1967). Problems arising from a large effective membrane impedance prevented the operation of the system with water flowing in one end of the sample and out the other, as was originally planned. Instead, the flow cell (Fig. 1) was operated as a double-sided pressure chamber. The 20-mm axial thickness was intended to be small enough that the normally sluggish response of a natural soil would be manageable.

Tensiometers and a gamma-ray transmission system (described by Herkelrath and Miller, 1976) were used to measure ψ and θ. The three tensiometers were positioned so that ψ at the midpoint of the sample as well as the vertical gradient of ψ could be measured. The gamma-ray beam was positioned to go through the center of the column. For optimum counting statistics with 0.66-MeV gamma rays, the column diameter was 150 mm.

A continuously changing water pressure $p(t)$ was applied to the top and bottom of the sample. Accordingly, pressure gradients developed, the central region lagging behind the top and bottom pressures. The magnitude of this gradient was usually <100 kPa/m for glass beads and sand, and >500 kPa/m for silt loam. Much smaller gradients were present when samples were near saturation. An attempt was made to calculate hydraulic conductivity from the matric potential gradient and the time rate of change of water content, but small gradients and "noisy" θ data made the results unreliable. For computations of ψ-θ relations, readings of the center tensiometer were used.

A flexible membrane assembly was developed and used on both ends of the sample. Figure 1 illustrates this device in assembled (top half) and exploded (bottom half) views. The membrane itself was a thin piece of wettable plastic filter material with an air-entry value of about 150 kPa (model HT-200, Gelman Inst. Co., Ann Arbor, MI).[3] Water was supplied to the membrane through a zig-zag groove pattern in a flexible polyurethane backing plate. To remove bubbles that would accumulate, water was circulated through the grooves continuously. A fine-mesh stainless steel screen supported the membrane over the grooves of the plate. All three layers of the membrane assembly were flexible, so that a pressure greater than that of the soil atmosphere applied behind the backing plate conformed the membrane to the shape of the soil surface. Rigid stainless steel disks (not shown in Fig. 1) were positioned behind each backing plate to support the membrane assembly during packing operations.

The polyurethane material used for the backing plates was Flexane 80 (Devcon Corp., Danvers, MA.), which unfortunately has soluble components that can significantly affect the surface tension of water. Rinsing the plates for a few days in a running-water bath greatly reduced the severity of this effect, though it still influenced the measurements to some extent. Table 1 shows values of surface tension, measured by the de Nouy ring method, for water exposed to Flexane at different temperatures. The quantity of water exposed in these measurements was 0.01 m^3 for each square meter of Flexane surface area. Some time after the experiments described in this paper were completed, Amir Saleh-

[3] Mention of specific brand names does not imply endorsement by the U.S. Geological Survey or the Univ. of Wisconsin.

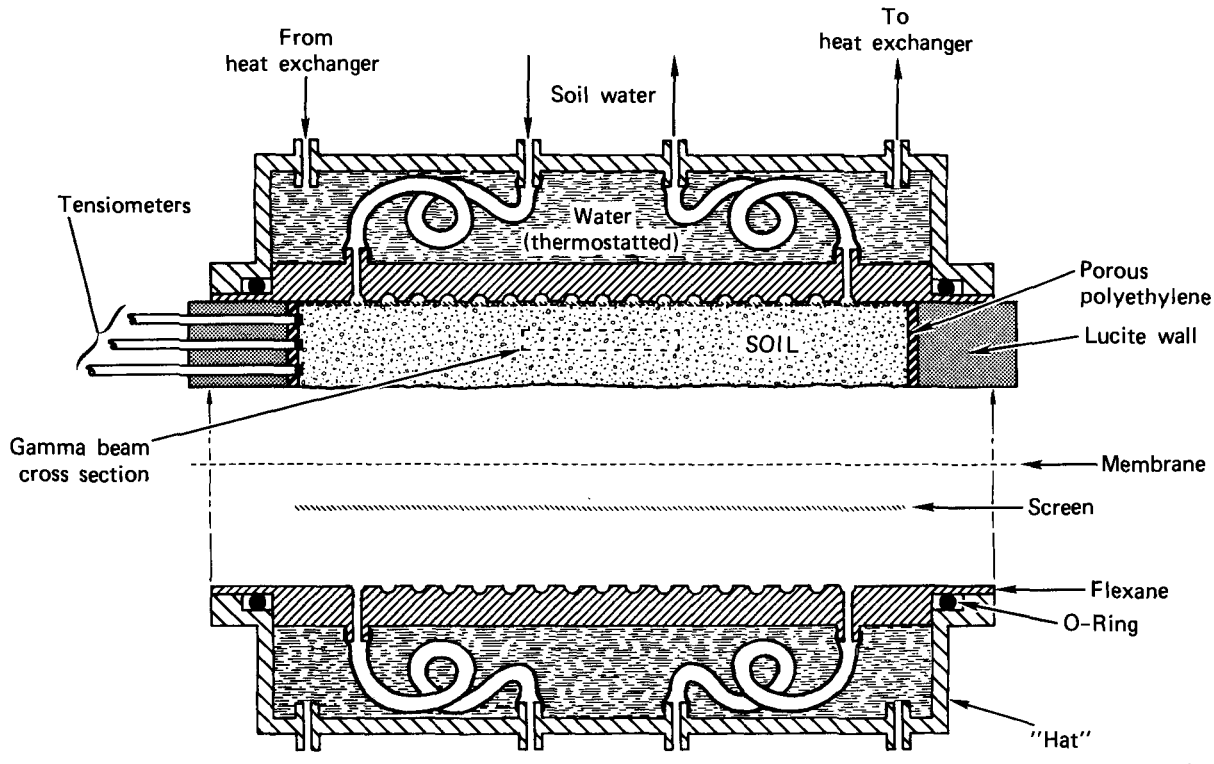

Fig. 1. Cross-sectional diagram of soil cell, approximately to scale, with the lower membrane assembly shown in exploded view. The indicated circulation of soil water is for bubble-sweeping; there is net outflow or inflow depending on whether the soil is drying or wetting.

zadeh found that the substitution of room-temperature vulcanizing (RTV) rubber for Flexane greatly reduces the problem of contaminant effects on surface tension.

The air pressure in the sample chamber was held constant by a regulator that was dead-end connected to the chamber through a hole in its wall. A 3-mm thickness of porous polyethylene lined the chamber to facilitate equilibration of air pressure throughout the cell. The water pressure $p(t)$ was controlled by an arrangement of regulators called the pressure programmer, a modification of an arrangement developed by Bomba (1967). Air was bled slowly out of (or into) a large air tank to produce a changing pressure that was transmitted to the soil water by means of a "sipper" regulator (Miller and Nimmo, 1986). A differential pressure regulator maintained a constant pressure drop across the bleed valve in order to produce a constant bleed rate and a linear $p(t)$.

To control the sample temperature, a thermostatted water bath was circulated in cylindrical chambers, referred to as "hats," behind each membrane-backing plate. This water, pressurized to maintain good membrane contact, was pumped continuously through a heat exchanger immersed in a bath with temperature controlled by a conventional thermoregulator. In each hat the flow was directed by a nozzle (not shown in Fig. 1) to produce vigorous circulation. The temperature-bath water was also pumped through Cu tubes attached to a thin Al band (not shown in Fig. 1) around the outer circumference of the sample chamber. To minimize gradients of temperature, the two hats and the Cu tubing were connected in parallel and the whole assembly was surrounded with thermal insulation.

During each experimental run $p(t)$ was varied according to a program designed to obtain the desired main and scanning curves. The rate of change of pressure depended on the medium, the time required to measure a single main curve being about 3000 s for glass beads, 9000 s for sand, and 12000 s for silt loam. Water content, matric potential, and temperature were measured every 10 s during each run and the data were stored on floppy disks using a microcomputer. For calibration, at about 2-h intervals, the pressure transducers were briefly switched to known reference pressures generated by water in standpipes. These measurements provided data for the slope and intercept values of the voltage-pressure relation. Reference gamma-counting rates (transmission through a lucite block used as a standard absorber) were also recorded about every 2 h. For the final calculation of ψ and θ, the calibration and reference data were interpolated linearly over time.

The first of the three porous media used in this experiment was a glass bead sample intended to duplicate the sample of Topp and Miller (1966). It was taken from the same batch of 181-μm spherical beads and was cleaned very thoroughly by the same procedures, involving treatment in strong solutions of sodium hydroxide and chromic acid. Packed under water as in the earlier experiments, the sample had a bulk density of 1.61 Mg/m^3 and a porosity of 0.350. Topp and Miller obtained a somewhat lower porosity of 0.326, probably because their sample chamber permitted more thorough vibration during packing. A second difference from the Topp and Miller experiment was that the newer apparatus, designed primarily for use with natural soils, could

Table 1. Measurements of the temperature dependence of the effect of Flexane 80 on the surface tension of water.

Temperature of exposure	Duration of exposure	σ after exposure
°C	min	mN/m
20.8	1	71.9
	18	51.8
	37	48.8
	103	46.6
	123	46.7
31.7	60	44.8
	102	42.9

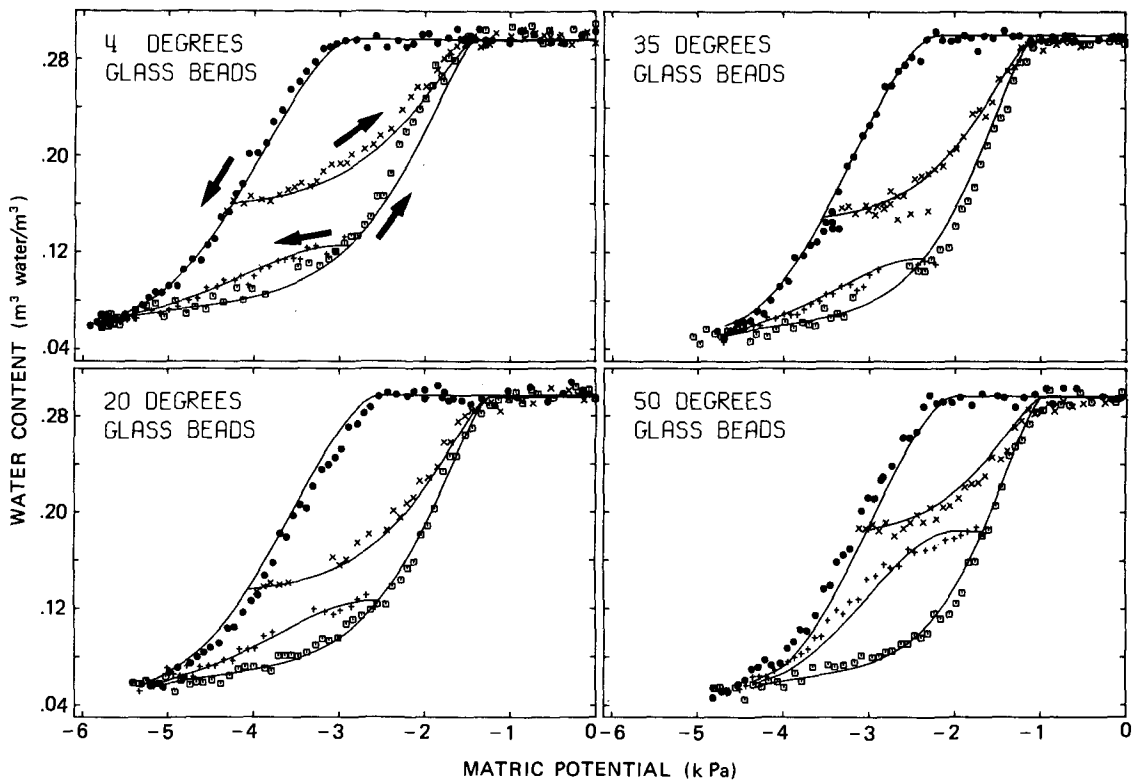

Fig. 2. Water content vs. matric potential for glass beads. The curves were computed using the gain-factor model of temperature dependence.

not be kept as free of trace contaminants that affect the surface tension of water. In comparing measured results with those of Topp and Miller, it should be noted that in the present experiment both the greater porosity and the lower surface tension would perturb the moisture retention curves in the direction of greater (less negative) values of potential.

The medium sand was taken from the same batch of surface-layer Plainfield loamy sand (sandy, mixed, mesic, Typic Udipsamments) that was used in the experiments of Jury and Miller (1974). It was packed under water to a bulk density of 1.69 Mg/m^3, compared to 1.67 Mg/m^3 for the sample of Jury and Miller.

The third sample, an undisturbed core of Plano silt loam (fine-loamy, mixed, mesic, Typic Argiudolls) from an apple orchard in Arlington, WI, was expected to have characteristics generally comparable to those found by Jaynes and Tyler (1980) and Baker and Bouma (1976) for the same series. The soil used in the experiment was from the A horizon at the 0.30-m depth. Further description of the experimental apparatus and media is given by Nimmo (1983).

RESULTS

For the three selected media the experimental plan required measurements of characteristics at four temperatures: 4, 20, 35, and 50°C. Each run comprised a main drying and main wetting cycle and two primary scanning curves, one drying and one wetting. The θ range was determined at the wet end by the rewet saturation condition (with entrapped air) and at the dry end by the point where tensiometer contact with the soil became unreliable.

Of the original plan for 12 data sets, two are missing: (i) the sand sample was accidentally destroyed before the 4° run could be completed, so these data do not exist, and (ii) results of the silt loam run at 20° were judged to be invalid because of inconsistency between segments of the run that should have been identical. Data from this run also showed flagrant deviations from the temperature trend established by data at 4, 35, and 50°C. For this soil the 20° measurements were made before the others, probably during the period of changing characteristics expected at the start of measurements on a new sample.

Figures 2 through 4 are graphs of the measured (ψ,θ) points, with smooth curves determined according to the "gain-factor" model described below. Not all data are shown, just the portions used in analyzing the temperature dependence. On the glass-bead graphs (Fig. 2) individual points represent measurements made at 10-s intervals, while on the sand and silt-loam graphs (Fig. 3 and 4) each point is the average of 10 data points taken during a 100-s period. The point symbols are solid circles for main drying curves, squares for main wetting curves, plus signs for scanning drying curves, and x's for scanning wetting curves. Some data points have been omitted for clarity. For each medium, a criterion for minimum spacing of displayed points was chosen and a point was eliminated wherever the ψ difference between two points was less than this criterion. The criterion was 0.06 kPa for glass beads, 0.05 for Plainfield sand, and 0.5 for Plano silt loam. Tables 2 through 4 indicate the sample temperatures and chronological order for all data segments.

Measurement errors were estimated by combining the effective errors from all known sources. For temperature the overall estimated error is ± 0.2°C. For ψ the error is ± 0.15 kPa for glass beads and sand and ± 1.4 kPa for silt loam. For θ measurements the random component of error, dominated by statistical fluctuations in output of the gamma source, is ± 0.004

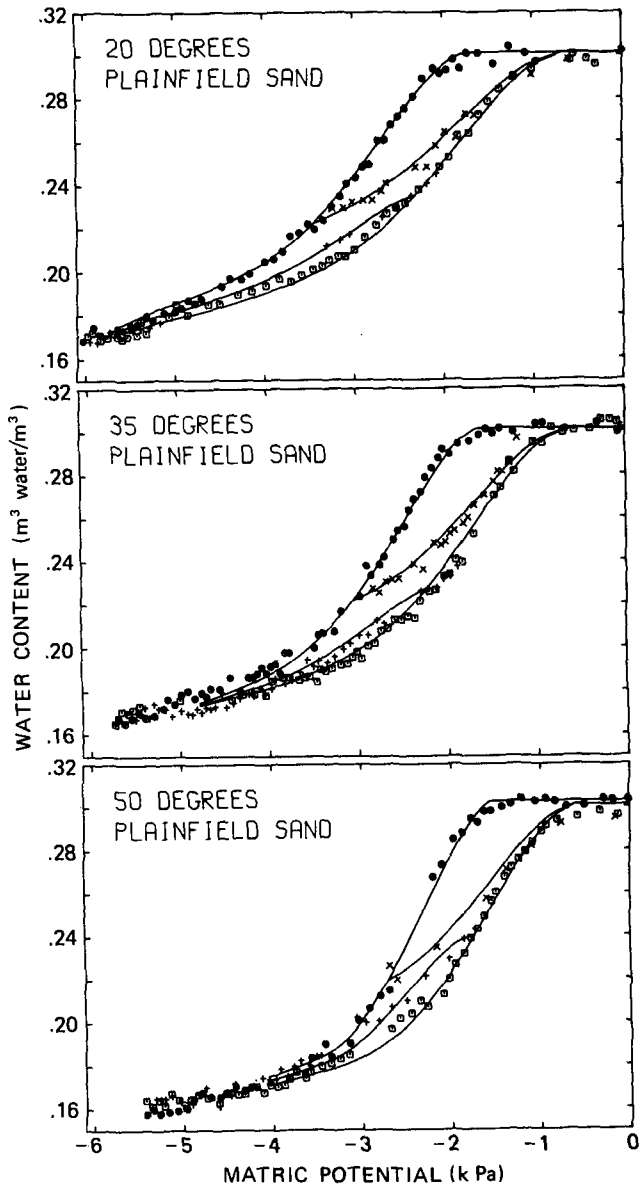

Fig. 3. Water content vs. matric potential for Plainfield sand.

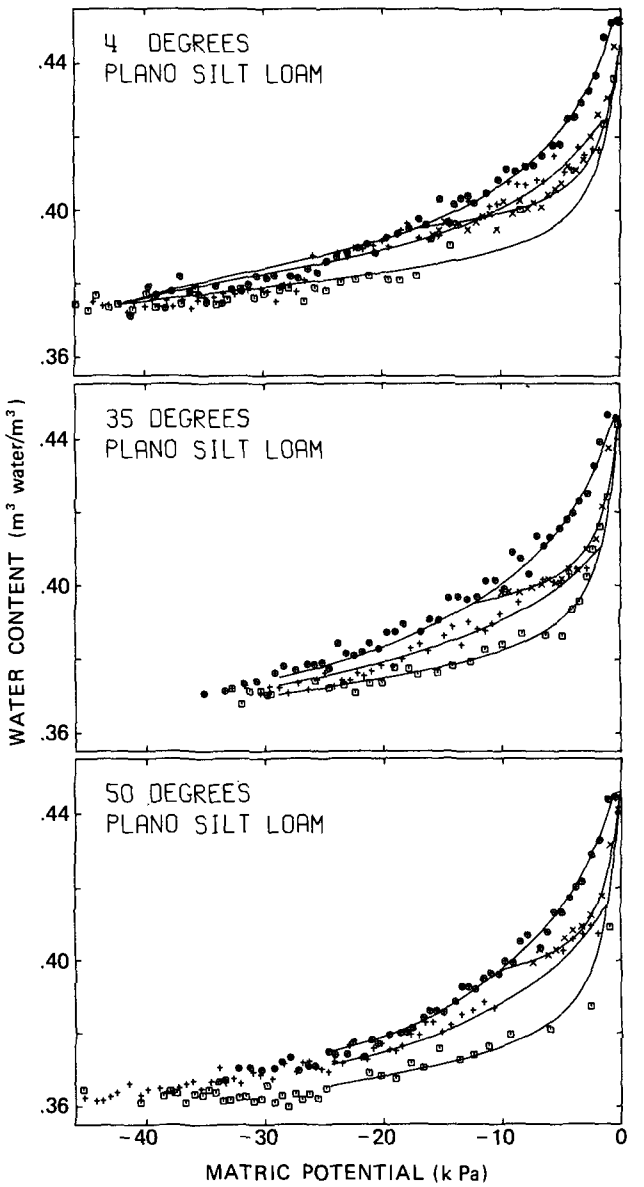

Fig. 4. Water content vs. matric potential for Plano silt loam.

m^3 H_2O/m^3 for the 10-s measurements on glass beads and ± 0.002 m^3 H_2O/m^3 for the 100-s measurements on sand and silt loam. The θ measurements are also subject to systematic errors, dominated by calibration discrepancies, that might be as large as 0.005 m^3 H_2O/m^3. Because only relative water contents enter into the analysis of temperature effects and hysteresis, only the random θ error needs to be considered for these purposes.

Analysis of Experimental Data

To derive a simple representation of temperature dependence from the experimental data, a model has been developed that is used in combination with an independent-domain hysteresis model of Mualem (1974), referred to in later papers as "Model II." In this hysteresis model two pore-size distribution functions, $L(\psi)$ and $H(\psi)$, are evaluated from main drying and wetting curves and represent (at a single temperature) all possible scanning curves within the envelope of the main curves. In the empirical model developed here, a third function, $G(\theta)$, represents the temperature dependence, G being the factor by which the STVF temperature dependence is exceeded. Once these three functions are determined from measured data, the combined model predicts any main or scanning curve at any temperature.

Before the measured points on the main curves could be used to compute the functions $L(\psi)$, $H(\psi)$, and $G(\theta)$, two operations were necessary. First, the "noisy" $\theta(\psi)$ points were fitted with one of several variations of a standard least-squares polynomial regression technique. Then these fitted curves were adjusted to compensate for the fact that they begin at different θ values (which would otherwise compound the apparent temperature dependence with hysteresis effects). Because each curve is determined by its starting point to be a single member of a family of possible curves, any two drying (or wetting) curves from the data sets of two

Table 2. Sample temperatures for glass beads, with the chronological rank of each segment indicated in parentheses below the temperature.

Nominal	Main drying	Main wetting	Scanning drying	Scanning wetting
		°C		
4	4.5 (7)	4.4 (9)	4.6 (8)	4.3 (10)
20	19.5 (4)	19.5 (6)	19.5 (5)	19.5 (3)
35	36.1 (1)	36.0 (12)	35.1 (11)	35.6 (2)
50	47.3 (13)	47.5 (15)	47.4 (14)	47.8 (16)

Table 3. Sample temperatures and chronological rank of data segments for Plainfield sand.

Nominal	Main drying	Main wetting	Scanning drying	Scanning wetting
		°C		
20	19.2 (10)	19.2 (12)	19.3 (11)	18.8 (9)
35	34.1 (2)	34.4 (4)	34.2 (3)	34.1 (1)
50	49.2 (5)	49.5 (7)	49.6 (6)	49.5 (8)

Table 4. Sample temperatures and chronological rank of data segments for Plano silt loam.

Nominal	Main drying	Main wetting	Scanning drying	Scanning wetting
		°C		
4	3.6 (11)	3.3 (12)	4.5 (9)	2.5 (10)
35	34.9 (4)	34.9 (2)	34.7 (1)	35.0 (3)
50	49.7 (6)	49.8 (8)	49.4 (7)	49.4 (5)

different temperatures will differ in part because of slight differences in starting point with respect to θ and in part because of temperature. Mualem's Model II was used to compute scanning curves very close to the measured curves, starting from the same θ value for each temperature. These adjusted curves were assumed to differ only because of the temperature difference, and were used as main drying and wetting curves in succeeding calculations.

The function $G(\theta)$ quantifies temperature dependence according to the definition

$$G(\theta) = \frac{\psi_j(\theta)/\psi_i(\theta) - 1}{\sigma_j/\sigma_i - 1} \qquad [2]$$

where the subscripts i and j refer to two temperatures T_i and T_j ($T_i > T_j$), $\psi_i(\theta)$ and $\psi_j(\theta)$ are curves based on experimental data (measured under conditions identical except for temperature), and σ_i and σ_j represent the surface tension of pure water. Since STVF scaling (Eq. [1]) indicates that for a given θ (and θ-history at a fixed temperature) $\psi(\theta)/\sigma$ should be independent of temperature, the ratio σ_j/σ_i is the STVF prediction of the ratio $\psi_j(\theta)/\psi_i(\theta)$. Thus the denominator of Eq. [2] is the STVF-predicted departure from unity of $\psi_j(\theta)/\psi_i(\theta)$ while the numerator is the actual departure. Equivalently, $G(\theta)$ may be thought of as the ratio of the actual difference $\psi_j(\theta) - \psi_i(\theta)$ to the STVF-predicted difference. It is important to maintain the convention that T_i be the greater of the two temperatures because a somewhat different value of $G(\theta)$ would be calculated otherwise.

Using a rearrangement of Eq. [2],

$$\psi_j'(\theta) = \psi_i(\theta)[1 + G(\theta)(\sigma_j/\sigma_i - 1)], \qquad [3]$$

a data curve $\psi_i(\theta)$ may be "translated" from temperature T_i to the equivalent curve $\psi_j'(\theta)$ at T_j. By translating the experimentally based curves to the same temperature T_o (4°C in this case) and then taking an arithmetic average, a composite is formed that serves as a standard $\psi(\theta)$ curve. An optimization procedure was developed to produce values of $G(\theta)$ and main drying and wetting standard curves for each medium, the $G(\theta)$ values being those that minimize the spread of the $\psi_o'(\theta)$ curves after translation to T_o. With the available experimental data for glass beads, Plainfield sand, and Plano silt loam, a $G(\theta)$ function could be found (Fig. 5) such that these translations to the standard temperature deviated from each other only slightly. The translated curves, the standard curves, and the original 4° data curves are nearly identical in appearance. The fact that this was true with data from three or four temperatures shows that $G(\theta)$ does not depend significantly on temperature over the range studied.

With two standard $\theta(\psi)$ curves (drying and wetting) and $G(\theta)$ available for each medium, model predictions were made for each measured curve. The first computational step was to translate the standard curves to the temperature of each experimental measurement. Then Mualem Model II was used to calculate main and scanning curves starting from the same points as the measured curves. For main curves this operation was an undoing of the previously described adaptation for unequal starting points, while for scanning curves it was an ordinary application of the model. Nimmo (1983) gives a detailed explanation of how these curves were computed.

The gain-factor model was used to compute the fitted main and scanning curves shown with the measured data points in Fig. 2 through 4. For a simple comparison, Fig. 6 shows optimized gain-factor fits, STVF fits, and the direct, least-squares fits to the experimental data. The least-squares method always gave close fits to the measured points, at least as close as any of the curves in Fig. 2 through 4, so these fits are useful as a standard of comparison. The STVF fits were computed in the same way as the gain-factor fits, but with $G(\theta)$ set equal to unity for the final translation. The comparison in Fig. 6 is made with main drying and wetting curves at 50°, since these have the largest span between the standard and computed curves and therefore provide the most demanding test of the models. In each case the gain-factor results fall much closer to the least-squares fits than do the STVF results.

The wiggles near the ends of the curves in Fig. 5 are not significant; in fact a straight line approximation to the computed $G(\theta)$ functions produces an adequate fit to the data points. The optimized $G(\theta)$ curves, in-

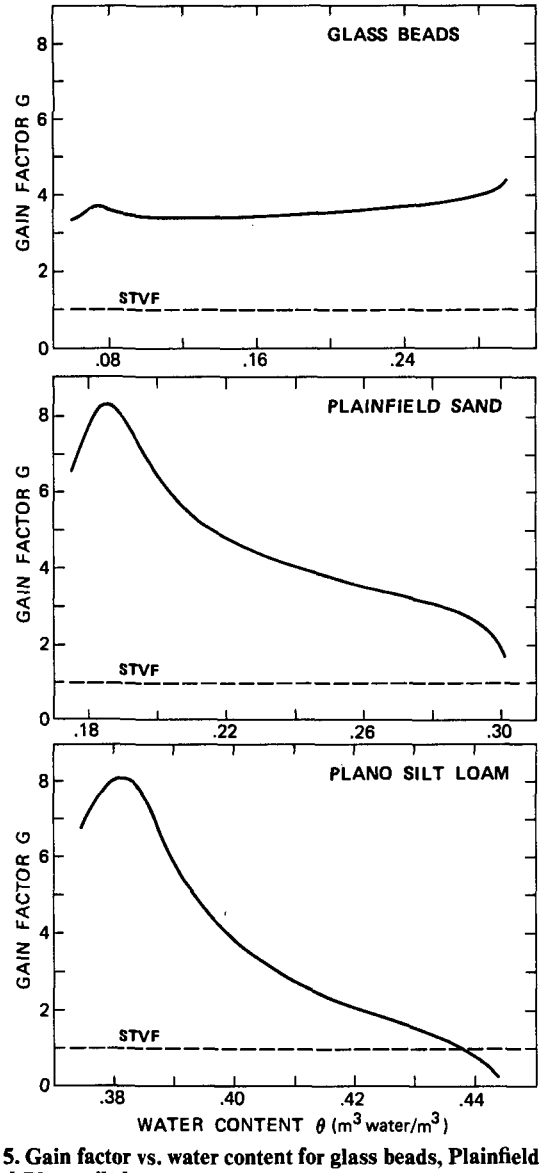

Fig. 5. Gain factor vs. water content for glass beads, Plainfield sand, and Plano silt loam.

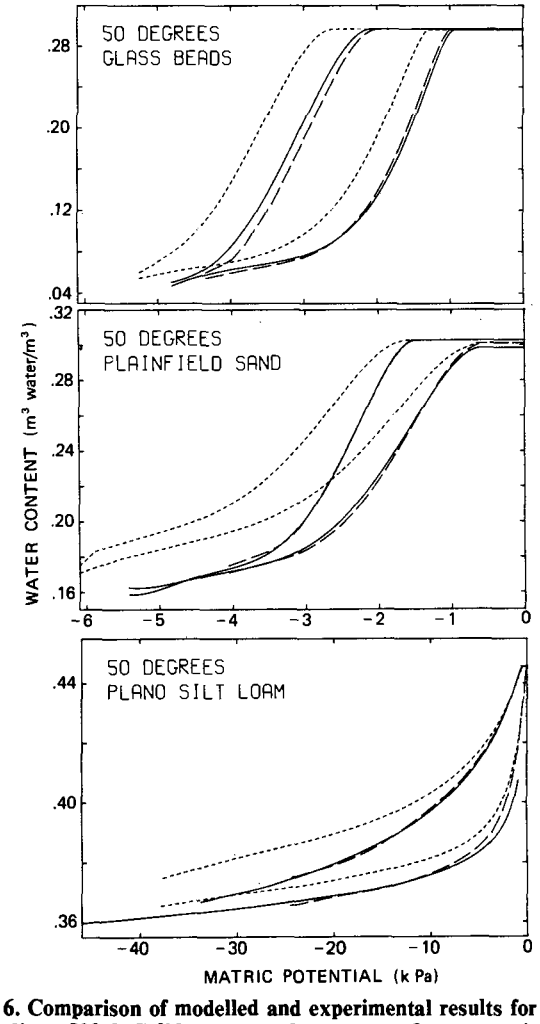

Fig. 6. Comparison of modelled and experimental results for three media at 50° C. Solid curves are least-square fits to experimental data, long-dashed curves are gain-factor calculations, and short-dashed curves are STVF calculations.

cluding wiggles, are presented because they are the direct result of the objective mathematical procedure described above.

To test whether there is a significant difference in the temperature dependence of drying and wetting, separate gain factors were computed, optimized for drying only, for wetting only, and for drying and wetting together. When these three different versions of the $G(\theta)$ function were used separately to produce curves corresponding to the experimental data, there was no significant difference in the quality of fit, as judged from visual comparison of the curves when graphed together.

DISCUSSION

The fit of the curves in Fig. 6 and 2–4 shows that the two functions from Mualem Model II (relating to pore-size distributions) combined with the gain-factor function (relating to temperature dependence) contain adequate information to reproduce main and scanning curves for the three different media over the 4 to 50°C range. The analysis shows that the temperature dependence of θ vs. ψ depends strongly on moisture conditions, but has nearly the same magnitude for different temperatures and for both drying and wetting. These facts suggest practical use of the model for predictions of $\theta(\psi)$ at any reasonable temperature, given measurements at as few as two temperatures. Further, the computed $G(\theta)$ curves are a valid basis for judging specific mechanisms of temperature dependence whenever theoretical gain factors can be estimated for comparison.

Some features of the gain-factor curves can be reasonably attributed to actual characteristics of the soil-water-air system while others result from experimental artifacts. For glass beads the measured $G(\theta)$ does not differ significantly from reasonable expectations based on artifacts such as contamination of the water by construction materials. From data in Table 1, the temperature dependence of surface tension for water contaminated by contact with the Flexane plates is estimated to produce a gain factor of about 3.3, not far from the values obtained for glass beads. For sand and silt loam, however, there are two features of the measured gain factors that known artifacts do not ex-

plain: (i) the large magnitude of $G(\theta)$ and (ii) the strong θ dependence of $G(\theta)$. Several hypotheses are commonly mentioned as explanations for a temperature dependence greater than the STVF model predicts, but most of these are inconsistent either with the measured gain factors or with the experimental conditions.

One hypothesis that could reasonably account for the observed gain factors is that the temperature dependence of the surface tension of soil solution is greater than that of pure water. In soils with organic matter, the water is known to contain surfactants such as fulvic and humic acid (Schnitzer and Desjardins, 1969; Chen and Schnitzer, 1978). Solutions of such fatty acids have been shown by Chen and Shnitzer and by Tschapek and Wasowski (1976) to have surface tensions as low as 44 mN/m (dyn/cm). If temperature variations somehow caused the surface tension of soil water to range between about 44 and 72 mN/m, the resulting gain factor might have a value of 5, not far from the values measured for sand and silt-loam samples. Such an enhanced temperature dependence of surface tension might occur (i) because of an increased concentration of surfactant at higher temperatures or (ii) because of an increase of effectiveness of surfactant at higher temperatures.

Two reports (Chen and Schnitzer, 1978; Tschapek et al., 1978) provide data on the surface tension of soil water from measurements made at 25°C. About 15 different soils that varied widely in organic matter content were included in the two studies. Chen and Schnitzer measured values ranging from 64.6 to 67.2 mN/m for water extracted from saturated soil pastes 1 h after the water and soil had been mixed. Tschapek et al. (1978) obtained estimates of 63 to 64 mN/m for saturated soil. The actual samples of Tschapek et al. were dilute slurries mixed in water/soil ratios of 1.5:1, 5:1, and 10:1. Measurements of σ were made 2 h after mixing and were extrapolated to estimate σ for a ratio equivalent to that of saturated soil (about 0.5:1).

The σ values measured for soil water are somewhat less than the 72 mN/m of pure water, but are considerably greater than the 44 mN/m measurement of fatty acid solutions mentioned above and are also greater than the 50 mN/m measurements that Chen and Schnitzer reported for water exposed to dried, powdered leaves. It is likely, then, that the concentrations of surfactant in the soil solutions were significantly less than the concentration at which the surfactants have their maximum effect (the critical micelle concentration, or CMC). Under these conditions variations in concentration may strongly affect σ.

Tschapek et al. (1978) found no significant relation between organic matter content and σ, as long as organic matter was not completely absent. Concentrations of surfactant thus are probably limited by some factor other than the amount of undissolved surfactant originally present in the soil. This actual limiting factor is of interest because it may be temperature dependent. One obvious consideration is solubility: data cited by Singleton (1960) indicate that the solubility of various fatty acids in water increases by a factor of 2 or 3 as temperature increases from 0 to 60°C. The possible significance of this mechanism is difficult to assess, however, because the identity of the surfactants and the chemical environment of the soil are not well known.

Rate-related processes might be important in limiting surfactant concentrations, because in the surface-tension measurements discussed above (as well as in our transient ψ-θ measurements) the residence time of water in the soil was limited. Either the rate of solvation or the rate of diffusion (from the region of the liquid-solid interface to the bulk solution or from the bulk solution to the gas-liquid interface) might influence the amount of surfactant effectively concentrated at the surface for a given duration of exposure. Both solvation and diffusion are strongly temperature-dependent and so might be responsible for a fairly large gain factor. Of course these effects would be less apparent in experiments with longer exposure times, in which the solvation and diffusion processes would have more nearly run their course. The gain factor might decrease with longer exposure, but available data are not applicable to this issue.

Even for a fixed concentration of surfactant, the temperature dependence of surface tension for soil water might be greater than that of pure water. Unfortunately, the reported work on the surface tension of soil solution does not include measurements made at different temperatures. For various concentrations of pure surfactants there are measurements of surface tension at various temperatures (Hudson and Pethica, 1967). The results show a temperature dependence of surface tension that increases with concentration, peaking just below the CMC with a value about five times greater than for pure water; at concentrations about 2 orders of magnitude less than the CMC this dependence is about twice as great as for pure water. This effect might easily lead to a gain factor of two or more by itself and might augment any temperature dependence caused by variations in surfactant concentrations.

The θ dependence of the sand and silt loam gain factors can be explained to some extent by variations in surfactant concentration. If rate-related processes, such as solvation and diffusion (acting for a finite time) limit the amount of surfactant in solution, then the concentration would be determined by the amount of water present for dilution. It is not clear whether the area of air-water interface or the volume of water would be the dominant factor in surfactant dilution, but considerations presented by Skopp (1985) indicate that the change of interface area with θ does not have an obvious direction and may be small in magnitude. If the volume of water governs the effective dilution, concentrations should be lower at higher θ values. Evidence for this hypothesis comes from Tschapek et al. (1978), who obtained markedly lower σ values for the 1.5:1 than for the 5:1 (water/soil) dilutions. This result indicates that the amount of water present, at least for the case of very high θ values, is an important factor governing the concentration of surfactant. Considering the effect of dilution on the gain factor, if $G(\theta)$ for the more concentrated soil solution at low θ values were 5, let us say, while for pure water it is 1, then at the intermediate surfactant concentration of a large θ, it should (for whatever enhancement mechanisms are

operating) have a value between 5 and 1. Although this sort of effect cannot be quantified from available experimental results, it is consistent with the observed trend of the gain factors with water content.

The hypothesis discussed here in detail—that the measured temperature dependence of soil-moisture characteristics results from variations in the concentration and the effectiveness of surfactants—is consistent with the gain factors obtained from sand and silt-loam data. Of course there are other hypothetical mechanisms (e.g., temperature effects on the rate of bubble formation from dissolved air) that cannot be ruled out, simply because the $G(\theta)$ they would produce cannot be realistically estimated. It is possible, however, to recognize the inadequacy of a number of suggested explanations (e.g., thermal effects on the swelling of clays) because the gain factors these mechanisms would produce are far less than those based on measurement.

REFERENCES

Baker, F.G., and J. Bouma. 1976. Variability of hydraulic conductivity in two subsurface horizons of two silt loam soils. Soil Sci. Soc. Am. J. 40:219–222.

Bomba, S.J. 1967. Hysteresis and time-scale invariance in a glass-bead medium. Ph.D. thesis. Univ. of Wisconsin-Madison. (Diss. Abstr. 68-7089).

Bouyoucos, G.J. 1915. Effect of temperature on some of the most important physical processes in soils. Mich. Agric. Exp. Sta. Tech. Bul. no. 22.

Briggs, L.J. 1897. The mechanics of soil moisture. U.S. Dep. Agric. Div. of Soils Bull. no. 10.

Cary, J.W. 1975. Soil water hysteresis: Temperature and pressure effects. Soil Sci. 120:308–311.

Chahal, R.S. 1964. Effect of temperature and trapped air on the energy status of water in porous media. Soil Sci. 98:107–112.

Chen, Y., and M. Schnitzer. 1978. The surface tension of aqueous solutions of soil humic substances. Soil Sci. 125:7–15.

Constantz, J. 1982. Temperature dependence of unsaturated hydraulic conductivity of two soils. Soil Sci. Soc. Am. J. 46:466–470.

Constantz, J. 1983. Laboratory analysis of water retention in unsaturated materials at high temperature. p. 147–164. *In* J.W. Mercer, et al. (ed.) Role of the unsaturated zone in radioactive and hazardous waste disposal. Ann Arbor Science. Ann Arbor, MI.

Crausse, P., G. Bacon, and S. Bories. 1981. Etude fondamentale des transferts couples chaleur-masse en milieu poreaux. Int. J. Heat Mass Transfer 24:991–1004.

Flócker, W.J., M. Yamaguchi, and D.R. Nielsen. 1968. Capillary conductivity and soil water diffusivity values from vertical soil columns. Agron. J. 60:605–610.

Gardner, R. 1955. Relation of temperature to moisture tension of soil. Soil Sci. 79:257–265.

Haridasan, M., and R.D. Jensen. 1972. Effect of temperature on pressure head-water content relationship and conductivity of two soils. Soil Sci. Soc. Am. Proc. 36:703–708.

Herkelrath, W.N., and E.E. Miller. 1976. High performance gamma system for soil columns. Soil Sci. Soc. Am. J. 40:331–332.

Hudson, R.A., and B.A. Pethica. 1967. The effect of temperature on micellar properties of some pure nonionic surfactants. p. 631–639. *In* J.Th.G. Overbeek (ed.) Chemistry, physics, and application of surface active substances. Gordon and Breach, New York.

Jaynes, D.B., and E.J. Tyler. 1980. Comparison of one-step outflow laboratory method to an in situ method for measuring hydraulic conductivity. Soil Sci. Soc. Am. J. 44:903–907.

Jury, W.A., and E.E. Miller. 1974. Measurement of the transport coefficients for coupled flow of heat and moisture in a medium sand. Soil Sci. Soc. Am. Proc. 38:551–557.

King, F.H. 1892. Fluctuations in the level and rate of movement of ground-water. U.S. Dep. Agric. Weather Bur. Bull. no. 5.

Meeuwig, R.O. 1964. Effects of temperature on moisture conductivity in unsaturated soil. Ph.D. thesis. Utah State Univ., Logan. (Diss. Abstr. 64-13747).

Miller, E.E., and R.D. Miller. 1956. Physical theory for capillary flow phenomena. J. Appl. Phys. 27:324–332.

Miller, E.E., and J.R. Nimmo. 1986. The "Sipper," a simple and accurate pressure regulator. Soil Sci. Soc. Am. J. (in press).

Mualem, Y. 1974. A conceptual model of hysteresis. Water Resour. Res. 10:514–520.

Moore, R.E. 1940. The relation of soil temperature to soil moisture: Pressure potential, retention, and infiltration rate. Soil Sci. Soc. Am. Proc. 4:61–64.

Nimmo, J.R. 1983. The temperature dependence of soil-moisture characteristics. Ph.D. thesis. Univ. of Wisconsin-Madison. (Diss. Abstr. 83-17041).

Peck, A.J. 1960. Change of moisture tension with temperature and air pressure: Theoretical. Soil Sci. 89:303–310.

Philip, J.R., and D.A. de Vries. 1957. Moisture movement in porous materials under temperature gradients. Trans. Am. Geophys. Union 38:222–232.

Richards, L.A. 1931. Capillary conduction of liquids through porous mediums. Physics 1:318–333.

Schnitzer, M. and J.G. Desjardins. 1969. Chemical characteristics of a natural soil leachate from a humic podzol. Can. J. Soil Sci. 49:151–158.

Singleton, W.S. 1960. Solution properties. p. 609–682. *In* K. Marley (ed.) Fatty acids. Interscience, New York.

Skopp, J. 1985. Oxygen uptake and transport in soils: Analysis of the air-water interfacial area. Soil Sci. Soc. Am. J. 49:1327–1331.

Taylor, S.A. 1958. The activity of water in soils. Soil Sci. 86:83–90.

Taylor, S.A. and G.L. Stewart. 1960. Some thermodynamic properties of soil water. Soil Sci. Soc. Am. Proc. 24:243–247.

Topp, G.C., and E.E. Miller. Hysteretic moisture characteristics and hydraulic conductivities for glass-bead media. Soil Sci. Soc. Am. Proc. 30:156–162.

Tschapek, M., and C. Wasowski. 1976. The surface activity of humic acid. Geochim. Cosmochim. Acta 40:1343–1345.

Tschapek, M., C.O. Scoppa, and C. Wasowski. 1978. The surface tension of soil water. J. Soil Sci. 29:17–21.

Vetterlein, E. 1968. Untersuchungen über den Einfluss der Temperature auf die kapillare Leitfähigkeit und Wasserbindung in Böden. Albrecht-Thaer-Archiv 12:385–400.

Wilkinson, G.E., and A. Klute. 1962. The temperature effect on the equilibrium energy status of water held by porous media. Soil Sci. Soc. Am. Proc. 26:326–329.